

Bursting during intermittency route to thermoacoustic instability: Effects of slow-fast dynamics

Cite as: Chaos **30**, 103112 (2020); <https://doi.org/10.1063/5.0005379>

Submitted: 20 February 2020 . Accepted: 18 September 2020 . Published Online: 12 October 2020

Shruti Tandon, Samadhan A. Pawar , Subham Banerjee, Alan J. Varghese, Premraj Durairaj, and R. I. Sujith 

COLLECTIONS

 This paper was selected as an Editor's Pick



View Online



Export Citation



CrossMark

ARTICLES YOU MAY BE INTERESTED IN

COVID-19 in the United States: Trajectories and second surge behavior

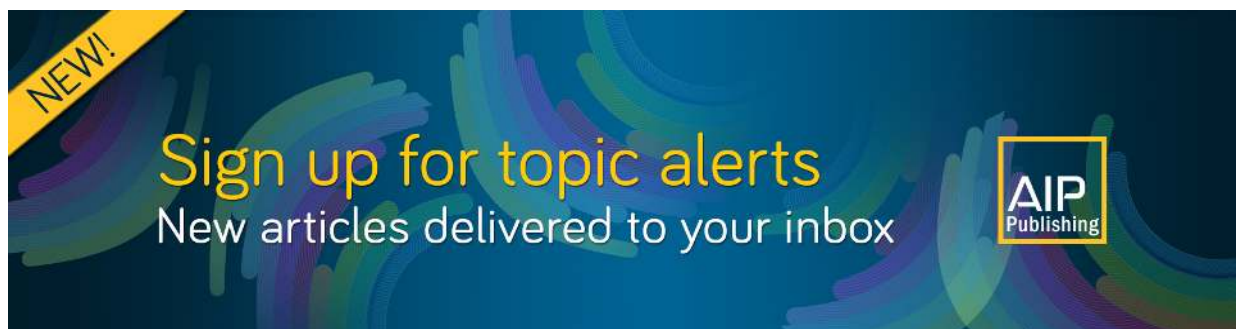
Chaos: An Interdisciplinary Journal of Nonlinear Science **30**, 091102 (2020); <https://doi.org/10.1063/5.0024204>

Abnormal route to aging transition in a network of coupled oscillators

Chaos: An Interdisciplinary Journal of Nonlinear Science **30**, 101101 (2020); <https://doi.org/10.1063/5.0022499>

Recurrence analysis of slow-fast systems

Chaos: An Interdisciplinary Journal of Nonlinear Science **30**, 063152 (2020); <https://doi.org/10.1063/1.5144630>



NEW!

Sign up for topic alerts
New articles delivered to your inbox



Bursting during intermittency route to thermoacoustic instability: Effects of slow-fast dynamics

Cite as: Chaos 30, 103112 (2020); doi: 10.1063/5.0005379

Submitted: 20 February 2020 · Accepted: 18 September 2020 ·

Published Online: 12 October 2020



View Online



Export Citation



CrossMark

Shruti Tandon, Samadhan A. Pawar,^{a)}  Subham Banerjee, Alan J. Varghese, Premraj Durairaj, and R. I. Sujith 

AFFILIATIONS

Department of Aerospace Engineering, Indian Institute of Technology Madras, Chennai 600036, India

^{a)} Author to whom correspondence should be addressed: samadhanpawar@gmail.com

ABSTRACT

Intermittency observed prior to thermoacoustic instability is characterized by the occurrence of bursts of high-amplitude periodic oscillations (active state) amidst epochs of low-amplitude aperiodic fluctuations (rest state). Several model-based studies conjectured that bursting arises due to the underlying turbulence in the system. However, such intermittent bursts occur even in laminar and low-turbulence combustors, which cannot be explained by models based on turbulence. We assert that bursting in such combustors may arise due to the existence of subsystems with varying timescales of oscillations, thus forming slow-fast systems. Experiments were performed on a horizontal Rijke tube and the effect of slow-fast oscillations was studied by externally introducing low-frequency sinusoidal modulations in the control parameter. The induced bursts display an abrupt transition between the rest and the active states. The growth and decay patterns of such bursts show asymmetry due to delayed bifurcation caused by slow oscillations of the control parameter about the Hopf bifurcation point. Further, we develop a phenomenological model for the interaction between different subsystems of a thermoacoustic system by either coupling the slow and fast subsystems or by introducing noise in the absence of slow oscillations of the control parameter. We show that interaction between subsystems with different timescales leads to regular amplitude modulated bursting, while the presence of noise induces irregular amplitude modulations in the bursts. Thus, we speculate that bursting in laminar and low-turbulence systems occurs predominantly due to the interdependence between slow and fast oscillations, while bursting in high-turbulence systems is predominantly influenced by the underlying turbulence.

Published under license by AIP Publishing. <https://doi.org/10.1063/5.0005379>

Large amplitude self-sustained oscillations in the acoustic field may arise due to positive feedback between the heat release rate and the pressure oscillations in a combustor. This phenomenon, known as thermoacoustic instability, has detrimental effects on the lifetime of a combustor. Recently, studies in many systems have shown that such thermoacoustic oscillations are preceded by a state of intermittency. In order to predict or mitigate these oscillations, it is essential to characterize the route to thermoacoustic instability and recognize its cause. During intermittency, bursts of high-amplitude periodic oscillations occur amidst epochs of low-amplitude aperiodic fluctuations. Such a dynamical state has been observed across various combustors, but the features of these bursts are different in different combustors. The cause of intermittent bursting is usually attributed to turbulent fluctuations in the underlying flow. However, intermittent bursts are also observed in laminar

and low-turbulence combustors, indicating a different physical cause. There are several subsystems in thermoacoustic systems such as the acoustics, flame dynamics, and hydrodynamics. We conjecture that the existence of the multiple timescales associated with the oscillations in these different subsystems in a thermoacoustic system is responsible for the occurrence of the bursts during intermittency, and the interaction between these oscillations determines the features of the bursts. To that end, we study the effect of multiple timescales on the occurrence of bursts in a prototypical thermoacoustic system using a horizontal Rijke tube. Furthermore, we present a phenomenological model to explain the cause of bursting in laminar and low-turbulence combustors through the framework of slow-fast systems. We also investigate the effect of the interaction between various subsystems on the characteristics of bursts observed during intermittency.

I. INTRODUCTION

Continuous combustion is required in several applications for power generation, such as aero-engines, rocket propulsion, and gas turbine engines. The operation and lifetime of combustors developed for such power generation are plagued by the phenomenon of thermoacoustic instability.^{1,2} During the occurrence of thermoacoustic instability, large amplitude self-sustained tonal sound waves arise as a result of mutual interaction between the unsteady heat release rate due to combustion and the unsteady acoustic field of the combustor.³ Identification of dynamical routes that lead to thermoacoustic instability and developing measures for predicting or mitigating such a state has been a field of intense research recently.^{4,5}

Traditionally, the onset of thermoacoustic instability has been viewed as a sudden transition from stable operation to unstable operation of the system. In the purview of dynamical systems theory, this transition is referred to as Hopf bifurcation^{6,7} and the state of thermoacoustic instability is considered to be a stable limit cycle.⁸ Nair *et al.*⁹ showed that the transition from stable operation (combustion noise) to unstable operation (thermoacoustic instability) in turbulent combustors is interspersed by a dynamical state called intermittency. Intermittency prior to thermoacoustic instability is a state consisting of bursts of high-amplitude periodic oscillations interspersed amongst epochs of low-amplitude aperiodic oscillations. In the intermittency signals, the epochs of periodicity increase as the system dynamics approaches the point of onset of thermoacoustic instability. Subsequently, several studies have reported the presence of intermittency prior to thermoacoustic instability in different combustors.^{10–15,52}

In a laminar thermoacoustic system consisting of a matrix burner, Kasthuri *et al.*¹⁶ showed the presence of bursting oscillations (switching of oscillations between bursts of periodic oscillations and a nearly quiescent state) and mixed-mode oscillations (characterized by periodic oscillations switching between two different amplitudes) prior to the onset of limit cycle oscillations. In addition, Weng *et al.*¹⁷ showed the existence of self-sustained beating dynamics arising due to fluctuations in the flame location in a Rijke-type burner with a laminar premixed flame. Therefore, while intermittent bursts are observed in both laminar and turbulent combustors, the characteristic features of such bursts are different in these combustors due to the difference in the preceding stable state. In laminar combustors, the intermittent bursts consist of periodic oscillations amidst epochs of quiescence and, hence, are referred to as “bursting oscillations.”¹⁶ However, in turbulent combustors, the intermittent oscillations consist of bursts of periodic oscillations interspersed by epochs of low-amplitude chaotic fluctuations and thus referred to as “intermittency”⁹ and not bursting oscillations.

Several attempts have been made to explain the transition from a state of stable operation to thermoacoustic instability via intermittency in various combustors. Using the framework of synchronization theory, Pawar *et al.*^{19,51} studied the coupling between the acoustic pressure and the heat release rate fields and showed that these fields undergo intermittent phase synchronization during the state of intermittency in thermoacoustic systems. Further, most studies attribute the occurrence of bursting during intermittency to the effects of the underlying turbulent fluctuations,⁴⁹ which are modeled either as stochastic forcing terms in the heat release rate^{20,50} or

stochasticity in velocities of the vortices that convect in a turbulent combustion chamber.²¹ On the other hand, a deterministic approach was presented by Seshadri *et al.*²² to explain the cause of intermittency, which was based on the feedback between the acoustic waves generated due to the localized heat release and the vortex shedding in the system. Although some understanding has been developed on the occurrence of intermittency in turbulent combustors, the aforementioned studies could not explain the causes and characteristics of bursts in laminar and low-turbulence combustors.

The kind of bursting behavior observed during intermittency prior to thermoacoustic instability in various combustors is remarkably different. Figure 1 shows the time series of such intermittent oscillations reported in some of the recent studies involving different type of combustors with varying levels of turbulence. For combustors having a high-turbulence intensity [Figs. 1(a)–1(c)] in the underlying flow field, the intermittent bursts are almost continuous in time with no distinct transition between epochs of periodic and aperiodic fluctuations. On the other hand, the intermittent oscillations observed in low-turbulence¹⁸ [Fig. 1(d)] and laminar¹⁶ [Fig. 1(e)] combustors show the occurrence of pronounced bursts of large amplitude as well as small amplitude periodic oscillations amidst very low-amplitude (nearly quiescent) aperiodic fluctuations. The intermittent oscillations in these systems are characterized by relatively smooth and regular variation in the amplitude envelope with distinct occurrence of growth and decay pattern for the bursts. Further, Fig. 1(f) shows self-sustained beating dynamics in a Rijke-type laminar burner,¹⁷ where the pressure oscillations show a regular transition between bursts of periodic oscillations and epochs of steady state. Clearly, the occurrence of intermittent bursts in the system shown in Figs. 1(d)–1(f) is not turbulence-induced and, hence, cannot be explained by earlier models based on turbulence.^{20,22} We endeavor to possibly fill this gap and provide a model to explain bursting behavior observed in low-turbulence combustors through a different approach.

Intermittent bursts may arise as a result of turbulent fluctuations in the flow that affect the heat release rate fluctuations as well as the acoustic fluctuations just prior to the onset of thermoacoustic instability. However, in the absence of high-intensity turbulence in the combustor, such bursting behavior is prone to arise due to interactions between the oscillations in the flow field, heat release rate, acoustics, etc. which have very distinct timescales. Recent experimental studies have provided insight into the interaction between the hydrodynamic and acoustic subsystems leading to bursting dynamics in thermoacoustic systems. Hong *et al.*²³ have shown that control parameters such as the equivalence ratio oscillate at a timescale much slower than the acoustic timescale when the system is close to the onset of thermoacoustic instability. In addition, Nair *et al.*⁹ have conjectured that intermittent bursts in turbulent combustors can arise if the acoustic subsystem is modulated by the hydrodynamics over slow timescales. Premchand *et al.*²⁴ have shown the presence of two dominant frequencies during the state of intermittency in a bluff-body stabilized turbulent combustor. They showed that the low-frequency peak in the amplitude spectrum of velocity fluctuations corresponds to the slow hydrodynamic timescale, while the high-frequency peak in the amplitude spectrum of the pressure fluctuations corresponds to the fast acoustic timescale.

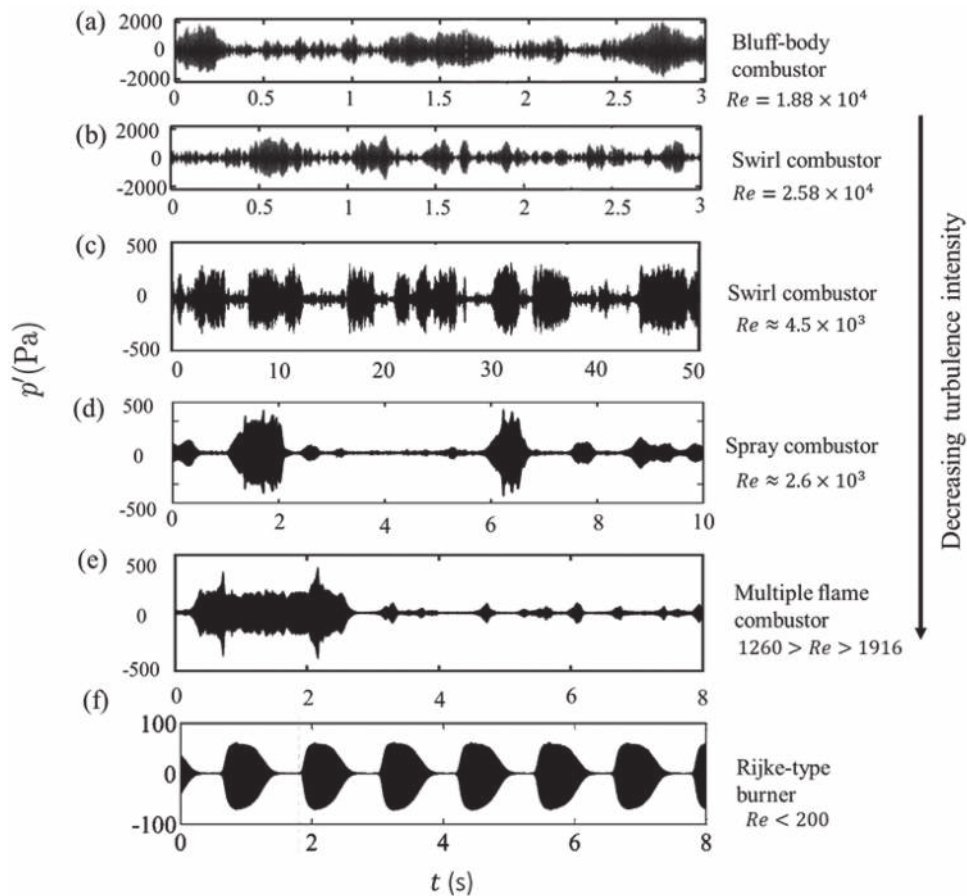


FIG. 1. The time series of the acoustic pressure oscillations during the state of intermittency observed prior to thermoacoustic instability obtained from studies involving different classes of thermoacoustic systems, such as [(a) and (b)] a turbulent gas-fired combustor with a bluff-body and a swirl stabilizer,⁹ respectively, (c) a turbulent gas-fired swirl combustor,¹⁵ (d) a low turbulence laboratory spray combustor,¹⁸ (e) a laminar multiple flame matrix burner,¹⁶ and (f) a Rijke-type laminar flame burner.¹⁷ These plots are reproduced with permission from: [(a) and (b)] Nair *et al.*, *J. Fluid Mech.* **756**, 470–487 (2014). Copyright 2014 Cambridge University Press; (c) Ebi *et al.*, *J. Eng. Gas Turb. Power* **140**, 061504 (2018). Copyright 2018 ASME; (d) Pawar *et al.*, *J. Eng. Gas Turb. Power* **138**, 041505 (2016). Copyright 2016 ASME; (e) Kasthuri *et al.*, *Chaos* **29**, 043117 (2019). Copyright 2019 AIP Publishing LLC; (f) Weng *et al.*, *Combust. Flame* **166**, 181–191 (2016). Copyright 2016 Elsevier.

Kasthuri *et al.*¹⁶ showed that the temperature close to the burner in a multiple flame combustor fluctuates at a slow timescale. They conjectured that the nonlinear interaction of the slow temperature oscillations and fast acoustic fluctuations gives birth to mixed-mode and bursting oscillations in their system. Further, Weng *et al.*¹⁷ conjectured that beating occurs in their system due to slow and fast timescales of the flame oscillations, where the slow timescale is around 100–1000 times the timescale of acoustic fluctuations induced in the system. Thus, all these studies provide an incentive to study the interaction of slow–fast dynamics in thermoacoustic systems, where the acoustic fluctuations are the fast subsystem while the slow subsystem is formed by the hydrodynamic oscillations or flame fluctuations. The hydrodynamic oscillations may further introduce slow oscillations in several other subsystems such as the heat release rate or the temperature, or in the control parameters such as the local equivalence ratio or the flow Reynolds number.

The occurrence of “bursts” is a widely studied phenomenon across numerous fields such as neuroscience,²⁵ chemical systems,²⁶ and fluid mechanics.²⁷ Across these numerous fields, bursting phenomena have been studied under the purview of coupling of slow and fast subsystems or multiple timescales associated with the system. Thus, bursting dynamics in thermoacoustic systems may also be studied in the purview of multiple timescales associated with the oscillations of various subsystems and control parameters. With the insight from experiments in thermoacoustic systems and studies from other fields as our motivation, we try to explain the cause of intermittency in low-turbulence systems using the slow–fast approach.

We conduct an experimental and theoretical investigation on a prototypical thermoacoustic system, known as the horizontal Rijke tube.²⁸ The horizontal Rijke tube inherently does not show intermittency or bursting behavior prior to the onset of thermoacoustic

instability.^{28–30} We design the experiments so as to create bursting behavior and, hence, to test the hypothesis of the occurrence of bursts due to multiple timescales in the Rijke tube. In pursuit of the same, we purposefully introduce sinusoidal oscillations in the control parameter (i.e., heater voltage) at a frequency which is orders of magnitude lesser than the acoustic frequency. The mean value of this oscillatory control parameter is varied such that the system dynamics transitions from steady state to limit cycle oscillations.

We also develop a low order phenomenological model with a canonical form for subcritical Hopf bifurcation for heat release rate fluctuations, where low-turbulence intensity is modeled using additive noise and interactions between various subsystems is modeled using multiplicative noise. Slow-fast dynamics is introduced in the model by the slow sinusoidal oscillation of the control parameter, in a similar manner as described for the experiments. Prior to thermoacoustic instability, we observe the occurrence of bursts of high-amplitude periodic oscillations amidst low-amplitude aperiodic oscillations in the acoustic pressure due to the slow modulations of the control parameter in the experiments on the Rijke tube as well as through our model. Finally, we study the interdependence of the various subsystems of a thermoacoustic system by two approaches in the model. In the first approach, we use the slow-fast systems approach and couple the oscillations of the slow and the fast subsystems, while in the second approach, we introduce multiplicative noise in the heat release rate term in the absence of slow oscillations in the control parameter. We show that a coupling between the slow and the fast subsystems induces regular amplitude modulations in the bursts of periodic oscillations, while the multiplicative noise introduces small and irregular modulations in the amplitude envelope of bursts.

II. EXPERIMENTAL SETUP

The experimental setup of a horizontal Rijke tube (Fig. 2) consists of an aluminum duct that is 100 cm long with a square cross section of $9.3 \times 9.3 \text{ cm}^2$. A decoupler is attached to the inlet of the duct. The decoupler eliminates the fluctuations of the incoming flow and maintains ambient pressure conditions at the attached side of the duct. The Rijke tube houses a stainless-steel wire gauge (henceforth, referred to as the heater), which is used as a concentrated heat source in the system. The heater is connected to a DC power supply (TDK-Lambda, GEN 8-400, 0-8 V, 0-400A) through two copper rods. The DC power supply is used to control the supplied voltage to the heater, which thus controls the amount of power supplied to the system. The heater voltage (i.e., the control parameter) is varied in a quasi-static manner such that the system dynamics transitions from the steady state to thermoacoustic instability (i.e., limit cycle oscillations) via a subcritical Hopf bifurcation. The airflow rate is maintained constant at $100 \pm 0.52 \text{ SLPM}$ (standard liters per minute), using an electronic mass flow controller (Alicat Scientific). The corresponding Reynolds number of the air flow in the Rijke tube is 1154 ± 6 .

To test our hypothesis on the occurrence of bursts due to slow-fast oscillations in a thermoacoustic system, we externally introduce slow timescale oscillations in the heater voltage. Such control parameter oscillations are introduced by generating a sinusoidal voltage signal using the SignalExpressTM software, which, in turn,

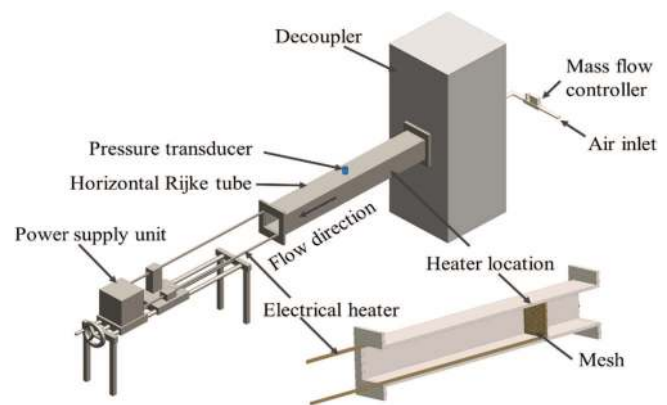


FIG. 2. The schematic of the experimental setup of the horizontal Rijke tube and a cross section of the Rijke tube duct showing the position of the heater in the system.

introduces sinusoidal oscillations in the heater power. Throughout all the experiments in the Rijke tube, the sinusoidal oscillations of the voltage supplied to the heater are maintained at an amplitude of 0.5 V and a frequency of 50 mHz. The mean value of the heater voltage is varied in the range 1.5–2.75 V, corresponding to which the mean value of the heater power varies in the range 200–600 W. In order to obtain bursting behavior in the system, we ensure that the frequency of the oscillations in the heater voltage is of the order of 1/1000th of the natural frequency of the acoustic oscillations developed during thermoacoustic instability in the Rijke tube, which is around 162 Hz. We use such a low ratio in order to allow enough decay and growth time between consecutive bursts of periodic oscillations in the acoustic pressure dynamics. Thus, the heater power oscillations reflect the slow subsystem, while the unsteady acoustic pressure fluctuations developed inherently in the system comprise the fast subsystem.

The unsteady acoustic pressure oscillations generated in the Rijke tube are recorded using a pressure transducer (PCB103B02), which has an uncertainty of $\pm 0.2 \text{ Pa}$. The transducer is located at a distance of 31.5 cm from the inlet of the Rijke tube. The sampling frequency was fixed at 10 kHz. The acoustic pressure data were collected using a 16-bit data acquisition system DAQ (NI-USB 6343). To ensure repeatability of the experimental results, environmental factors such as temperature and relative humidity were maintained at $23 \pm 3 \text{ }^\circ\text{C}$ and $60 \pm 5\%$, respectively. The acoustic decay rate of the setup under cold flow conditions was always recorded to be between $12 \pm 0.5 \text{ s}^{-1}$. The acoustic damping is maintained within bounds to ensure repeatability of the experiments.

III. MODEL BASED ON THE NORMAL FORM OF SUBCRITICAL HOPF BIFURCATION

In general, any thermoacoustic system consists primarily of a source of unsteady heat release subjected to an acoustic field established in a confinement. If the premixed/diffusion flame inside the duct is restricted to a smaller length compared to the size of the duct, it can essentially be considered as a concentrated source of heat,

just like the electrically heated wire mesh in the case of a horizontal Rijke tube. We, therefore, use a model similar to that discussed by Gopalakrishnan *et al.*,³¹ which is a modified form of the non-linear model developed by Balasubramanian and Sujith,³² to obtain subcritical Hopf bifurcation through a generalized heat release rate function.³³

A. Governing equations

The linearized non-dimensional equations for momentum and energy in one-dimension, neglecting the effect of mean flow and temperature gradient, are as follows:^{32,34}

$$\gamma M \frac{\partial u'}{\partial t} + \frac{\partial p'}{\partial x} = 0, \tag{1}$$

$$\frac{\partial p'}{\partial t} + \gamma M \frac{\partial u'}{\partial x} = (\gamma - 1) \dot{Q}' \delta(x - x_j), \tag{2}$$

where γ is the ratio of specific heat capacities, M is the mean flow Mach number, \dot{Q}' is the fluctuating heat release rate at the location of the heat source (x_j) in the system, while p' and u' are the fluctuations in the acoustic pressure and the acoustic velocity, respectively. Here, t denotes time and x denotes the distance along the axial direction of the duct. The set of partial differential equations (1) and (2) are converted to a set of ordinary differential equations (ODEs) by using the method of modal expansion, also often called the Galerkin projection.³⁵ Accordingly, we expand the acoustic pressure and velocity fluctuations as a linear combination of basis functions that satisfy the boundary conditions associated with the Rijke tube duct, which is open at both ends. Since, at open ends, the acoustic pressure fluctuations are zero and the acoustic velocity fluctuations are maximum, sine and cosine functions are a natural choice as basis functions for the modal expansion of p' and u' , respectively. The pressure and velocity fluctuations are expressed in terms of time-varying modes η and $\dot{\eta}$ as follows:

$$u'(x, t) = \sum_{j=1}^{\infty} \eta_j(t) \cos(j\pi x)$$

and

$$p'(x, t) = - \sum_{j=1}^{\infty} \frac{\gamma M}{j\pi} \dot{\eta}_j(t) \sin(j\pi x). \tag{3}$$

Substituting the expressions from Eq. (3) into Eqs. (1) and (2) and projecting the resulting equation on the j th mode of the basis function, we obtain the set of ordinary differential equations (ODEs) as given in Eqs. (4) and (5). Finally, we include the effect of damping in Eq. (2) by adding a damping term which is dependent on the frequency of the system,²⁸

$$\frac{d\eta_j}{dt} = \dot{\eta}_j, \tag{4}$$

$$\frac{d\dot{\eta}_j}{dt} + 2\varepsilon_j \omega \dot{\eta}_j + \omega^2 \eta_j = \dot{q}', \tag{5}$$

where ω is the non-dimensional angular frequency, \dot{q}' is the non-dimensional heat release rate term. Here, ε_j is the damping coefficient which is calculated according to the following equation, with

$k_1 = 0.1$ and $k_2 = 0.06$:

$$\varepsilon_j = \frac{1}{2\pi} \left(k_1 \frac{\omega_j}{\omega_1} + k_2 \sqrt{\frac{\omega_1}{\omega_j}} \right), \tag{6}$$

where $\omega_j = j\pi$ for the j th duct mode.^{28,36}

For a horizontal Rijke tube, the model developed by Balasubramanian and Sujith³² uses a modified form of King's law^{37,38} to model the heat release rate term (\dot{Q}'). King's law governs the heat release rate from the thin hot wire to the surrounding fluid, which is appropriate to describe the heat transfer from the electrically heated wire mesh to the air in the Rijke tube. However, for thermoacoustic systems in general, King's law may not be the most general description of the heat source as it is for a Rijke tube with electric heater.

For the current study, the non-dimensional heat release rate fluctuations are decomposed into coherent and non-coherent components in Eq. (7), as suggested by Noiray.²⁰ The coherent fluctuations in the heat release rate (\dot{q}'_c) are due to the interaction of the acoustic field fluctuations with the flame, while the non-coherent heat release rate fluctuations (\dot{q}'_{nc}) occur due to the turbulence in the underlying flow field,

$$\dot{q}' = \dot{q}'_c + \dot{q}'_{nc}. \tag{7}$$

The non-coherent component of the heat release rate, \dot{q}'_{nc} , is modeled using the noise term $\xi(t)$ in Eq. (8). The coherent heat release rate \dot{q}'_c is considered to be a nonlinear function of the non-dimensional acoustic modes η and $\dot{\eta}$. For the current study, we use the canonical form of the subcritical Hopf bifurcation for \dot{q}'_c with a time delay coupling between η and $\dot{\eta}$, as motivated by Gopalakrishnan *et al.*,³¹ which is given by Eq. (8),

$$\dot{q}'_c = -c_1(\eta - \tau \dot{\eta}) - c_3(\eta - \tau \dot{\eta})^3 + c_5(\eta - \tau \dot{\eta})^5 \quad \text{and} \quad \dot{q}'_{nc} = \xi(t), \tag{8}$$

where c_1 , c_3 , and c_5 are constants, and τ is the time delay term. As discussed by Gopalakrishnan *et al.*,³¹ the time delay term ensures that the heat release rate responds to the velocity fluctuations at the location of the heating source with a certain time delay. Furthermore, the heat release rate introduces nonlinear feedback between the evolution of acoustic pressure and acoustic velocity fluctuations. The specific expression of \dot{q}'_c in Eq. (8) also ensures that a subcritical Hopf bifurcation [Fig. 3(b)] is obtained for the set of ODEs (4) and (5).

The term $\xi(t)$ is a combination of multiplicative and additive noise. A random term [ξ_a in Eq. (9)] is added at each iterative step to the acoustic pressure fluctuations, to effectuate additive noise (strength σ_a) in the system. Similarly, we generate multiplicative noise of strength σ_m by adding a random term [ξ_m in Eq. (9)] to the acoustic pressure oscillations at each step, where the strength of the random term is directly proportional to $\dot{\eta}$ as noted in Eq. (9). Both the random terms ξ_a and ξ_m are generated by the Weiner process and are white Gaussian noise terms. The non-dimensional strengths σ_a and σ_m are a fraction comparable to the maximum amplitude of the non-dimensional pressure variable $\dot{\eta}$, which is of the order of 1 ($\dot{\eta} \sim 1$). These non-dimensional strengths are varied to simulate the absence of turbulent fluctuations ($\sigma_a = 0.0001$) and also low or high levels of turbulence or perturbations from other subsystems (where σ_a and σ_m are of the order of 0.1). We choose such an order of magnitude for the noise intensities, so that the ratio

of amplitudes of periodic and aperiodic oscillations in the acoustic pressure signal obtained from the model is similar to that obtained from experiments,

$$\xi(t) = \sigma_a \xi_a + \sigma_m \dot{\eta}(t) \xi_m. \tag{9}$$

A slow-fast system is formed by the two-way interaction of both the slow and the fast subsystems. The evolution of each subsystem is, in general, dependent on the other. To study slow-fast oscillations in a thermoacoustic system where the pressure fluctuations have a fast timescale, we introduce slow sinusoidal oscillations in the control parameter c_1 [Eq. (8)] centered at a mean value A , amplitude B , and frequency f . As stated earlier for the experiments, we maintain the value of the frequency of the control parameter in the model at an order of magnitude of 1/1000th of the natural frequency of the acoustic fluctuations (fast timescale). The oscillations in the non-dimensional control parameter c_1 are governed by the following equation [Eq. (10)]:

$$c_1 = A + B \sin(2\pi ft). \tag{10}$$

The set of ordinary differential equations, Eqs. (4) and (5), are solved by the stochastic Runge-Kutta method³⁹ for the heat release rate function given by Eqs. (7) and (8), subject to noise [as given in Eq. (9)] and control parameter oscillations of the form shown in Eq. (10). In the rest of the paper, we refer to the above model as the “standard model.” We also assume that the evolution of the control parameter (slow subsystem) stays independent of the dynamics of the acoustic field variables (fast subsystem), say, p' in the system in Sec. IV. Further, we investigate the effect of the evolution of fast subsystem on the evolution of the slow subsystem by introducing an

interdependence between the two subsystems, which is discussed in detail in Sec. V.

IV. RESULTS AND DISCUSSION

A. Bifurcation diagram

We plot the bifurcation diagram of the acoustic pressure oscillations obtained during the transition to thermoacoustic instability through experiments in the horizontal Rijke tube and the model. The bifurcation diagrams [Figs. 3(a) and 3(b)] show the variation of root mean square value (rms) of the acoustic pressure (p'_{rms}) with a quasi-static change in the heater power (or heater voltage) for the experiments and the non-dimensional parameter c_1 for the model, respectively. The non-dimensional acoustic pressure from the model is converted to a dimensional form by multiplying it with the atmospheric mean pressure for the ease of comparison with the experimental results. Since this is a phenomenological model, we aim only for a qualitative match with the experiments. The bifurcation diagrams shown in Figs. 3(a) and 3(b) are for laminar flow ($Re = 1154 \pm 6$) conditions in the experiment and very low noise intensity in the model ($\sigma_a = 0.0001$ to account for inherent noise in real systems), respectively.

When the control parameter value is varied in a quasi-static manner in the forward direction (i.e., the value of control parameter is increased), we notice a sudden transition of the system behavior from steady state to limit cycle oscillations at the Hopf bifurcation point H in Figs. 3(a) and 3(b). A further increase of the control parameter beyond the point H leads to a continuous increase in the amplitude of the limit cycle oscillations in the system. In the reverse direction, as the value of the control parameter is reduced,

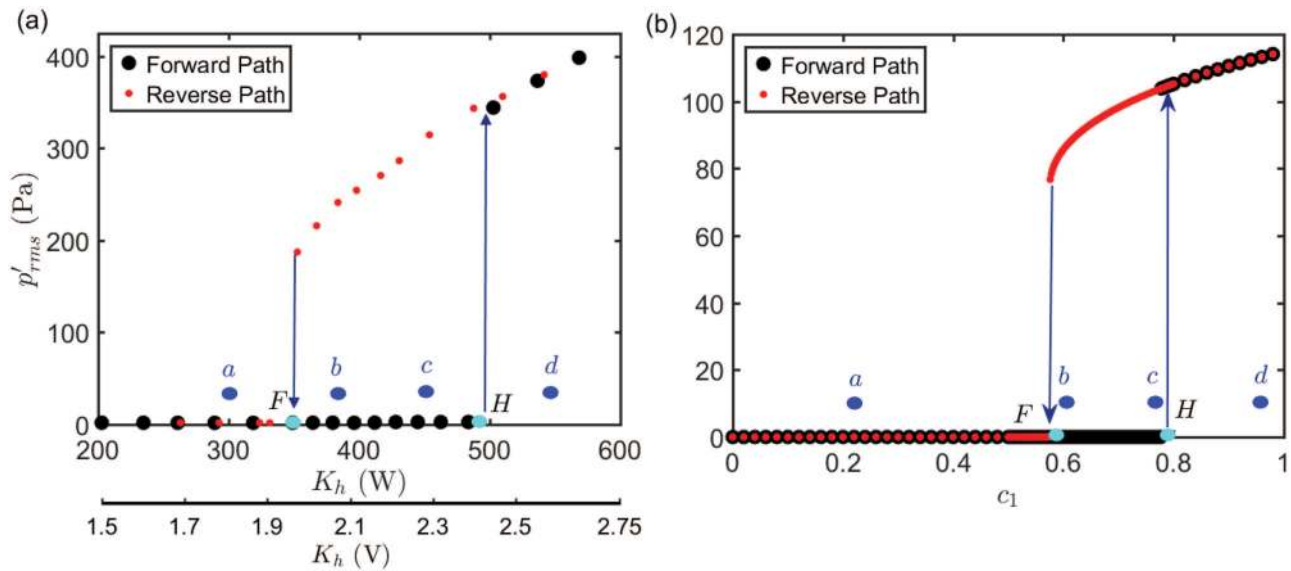


FIG. 3. The bifurcation diagram of the acoustic pressure fluctuations (p') with respect to (a) K_h , the heater power (W) or heater voltage (V) from experiments in the Rijke tube and (b) non-dimensional parameter c_1 from the standard model, when $\sigma_a = 0.0001$, $\sigma_m = 0$ in Eq. (9), $c_3 = c_5 = 1$ in Eq. (7). Points F and H represent the fold and the Hopf point, respectively, while a , b , c , and d are reference points.

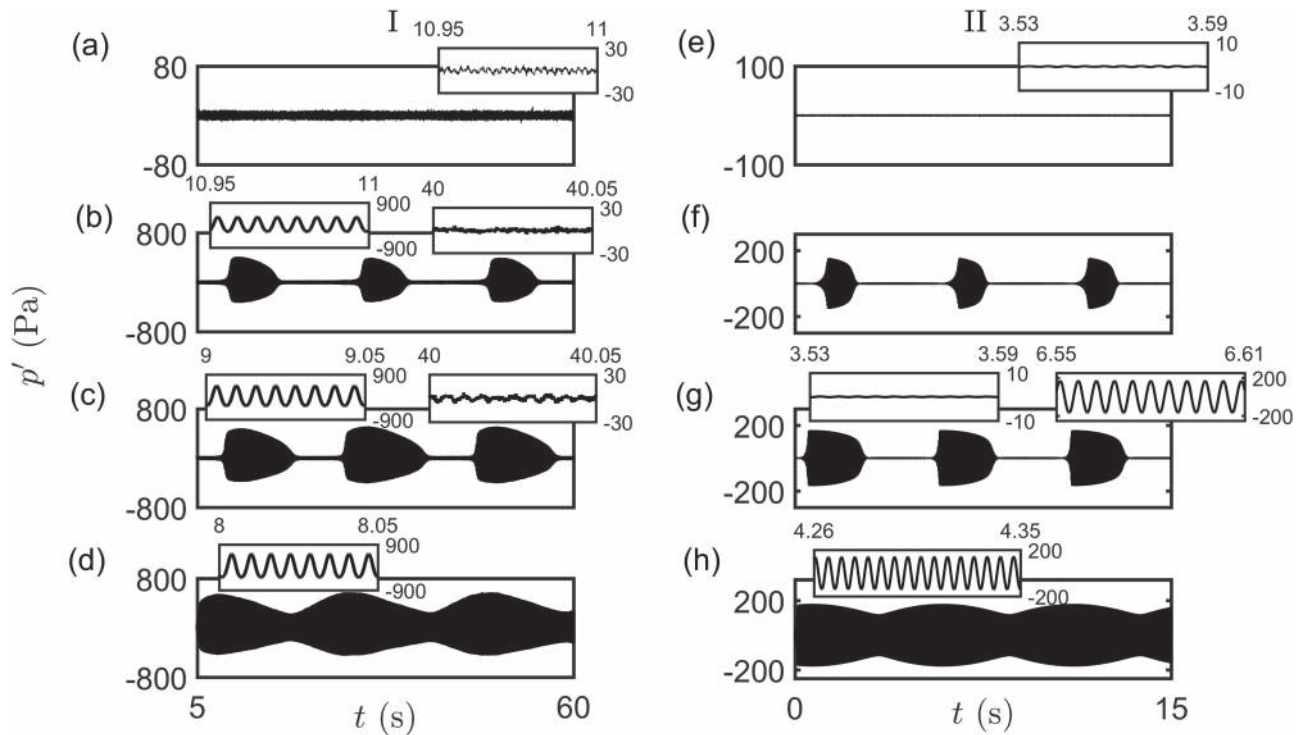


FIG. 4. Comparison of the time series of acoustic pressure (p') obtained from experiments (I) and from the model (II) for slow-scale oscillations in the control parameter about a mean value. For experiments, the mean value of K_h is varied from (a) to (d) as 1.8 V (306 W), 2.1 V (365 W), 2.2 V (428 W), and 2.56 V (568 W), respectively, where the amplitude and frequency of oscillations of K_h are fixed at 0.5 V and 0.05 Hz throughout. In the model, the parameter c_1 oscillates with amplitude $B = 0.4$ and frequency $f = 0.17$ Hz when its mean value is increased from (e) to (h) as $A = 0.2, 0.6, 0.75$ and 0.95 , respectively. The noise intensity in the model is $\sigma_a = 0.0001$.

we notice a continuous decrease in the amplitude of limit cycle oscillations, along the same path as in the forward direction. However, the transition from limit cycle to stable equilibrium state in the reverse direction occurs at point F (i.e., fold point), which is well past the point H . Thus, the bifurcation diagram exhibits a hysteresis region, indicative of a subcritical Hopf bifurcation in the system dynamics. In experiments, the Hopf bifurcation point is found to be at 2.45 V (483.6 W) and the fold point at 1.95 V (352.6 W). From the model, the Hopf and the fold point values for the non-dimensional parameter c_1 are 0.77 and 0.57, respectively, when we choose $\tau = 0.2$ and $c_3 = c_5 = 1$. Also, the bifurcation diagram in Fig. 3 is marked with points a, b, c , and d representing different dynamical states for reference in Fig. 4.

B. Effect of slow oscillations in the control parameter on the transition to thermoacoustic instability

In this section, we present the results of experiments on the horizontal Rijke tube, which were designed to investigate the occurrence of bursting oscillations induced due to the slow oscillations of the control parameter during the transition from steady state to limit cycle oscillations in the system. Figures 4-I and 4-II show the time series of acoustic pressure fluctuations from the experiments performed on the Rijke tube and from the model, respectively, for

the reference points of the subcritical Hopf bifurcation shown in Fig. 3.

Column I in Fig. 4 shows results from the experiments in the Rijke tube when slow oscillations, with fixed amplitude (0.5 V) and frequency (0.05 Hz), are induced in the heater voltage (K_h). The mean value of the heater voltage is increased from point a to d [with reference to the bifurcation diagram in Fig. 3(a)] in Figs. 4(a)–4(d), respectively. For oscillations about the mean value of K_h corresponding to a point in the steady state region, we observe only very low-amplitude aperiodic fluctuations, which can be considered as a quiescent state. As the mean value of the control parameter is increased to a value around the fold point [point b in Fig. 3], we observe bursts of high-amplitude periodic oscillations amidst nearly quiescent state, as seen in Fig. 4(b). We also obtain such bursting dynamics [Fig. 4(c)] when the mean value of the control parameter is in the bistable zone [point c in Fig. 3]. Comparing Figs. 4(b) and 4(c), we note that as the mean value of K_h is increased, the average epoch of the rest state reduces and the maximum amplitude achieved by periodic oscillations in the pressure signal increases. Finally, corresponding to control parameter oscillations about a point far ahead of the Hopf bifurcation point in the limit cycle regime [point d in Fig. 3], we observe the occurrence of limit cycle oscillations with modulated amplitude envelope, as shown in Fig. 4(d). Such modulations in the amplitude envelope arise when the minimum

value of the control parameter oscillations is more than or close to (if less than) the value of the control parameter at the fold point. That is, even though the control parameter oscillations may cross the fold point by a small margin and transit to the steady state region, the acoustic pressure oscillations never achieve a quiescent state. This is because the acoustic pressure oscillations in the active state have insufficient time to decay to the rest state, when a lesser fraction of the oscillation cycle of the control parameter occurs in the steady state region of the bifurcation diagram.

In column II of Fig. 4, we show the time series of acoustic pressure fluctuations obtained from the standard model (discussed in Sec. III) in the presence of slow timescale oscillations of the control parameter c_1 , as indicated by Eq. (10). The mean value (A) of the oscillating control parameter is increased in a quasi-static manner from point a to d [with reference to Fig. 3(b)] to obtain the dynamics shown in Figs. 4(e)–4(h). The model qualitatively captures all the features of bursting oscillations observed from experiments in the Rijke tube [Fig. 4-I]. The acoustic frequency of limit cycle oscillations obtained from the standard model is $f_a = 170$ Hz. In the absence of random perturbations (i.e., for $\sigma_a = \sigma_m = 0$) in the model, when the control parameter oscillations are introduced, we observe bursting behavior only when the mean value of the oscillating control parameter is greater than that at the Hopf bifurcation point. However, from the experiments in the Rijke tube, we observe bursting behavior even when the control parameter oscillations are centered much before the Hopf bifurcation point (i.e., in the bistable zone) [for example, see Fig. 4(b)]. This is because noisy fluctuations are inherent to any real system; hence, we use very low noise intensity ($\sigma_a = 0.0001$) to mimic such a noise in real systems. As a result, we obtain bursting behavior even when the control parameter is centered around the fold point, given that the amplitude of its oscillations is sufficient to cross the Hopf bifurcation point [for example, see Fig. 4(f)].

Similar to the experiments, the model produces bursts of high-amplitude periodic oscillations amidst nearly quiescent state [Figs. 4(f)–4(g)] and modulated limit cycle oscillations [Fig. 4(h)].

We also notice that such bursting behavior occurs only when the control parameter value crosses both the Hopf and the fold points in every cycle of the oscillation. Further, for the bursts induced by slow parameter oscillations (as shown in Fig. 4), we note that the transition from the rest to the active state (growth) and from the active to the rest state (decay) is asymmetric. A similar asymmetry in the growth and decay of the bursts of acoustic pressure signal has been recently reported in a Rijke-type burner by Weng *et al.*¹⁷ They observed that the asymmetry associated with bursting oscillations changes with the change in the equivalence ratio in the system; however, the cause of such asymmetry in a burst is not clear. In Sec. IV C, we try to explain this asymmetry of growth and decay of bursts with the help of the model discussed in Sec. III.

C. Delayed bifurcation effect

In this section, we discuss the reason for asymmetry in the growth and the decay pattern in the bursts induced by slow-fast dynamics in the experiments and the model [Fig. 4]. We believe that such asymmetry occurs due to the disproportionate time duration for which the system dynamics is restricted to the stable limit cycle branch during the forward and the reverse oscillation paths of the control parameter. Such unequal durations arise due to two reasons: (I) delayed bifurcation caused by the slow-scale oscillations of the control parameter and (II) the existence of a hysteresis zone in the bifurcation diagram of the system. The effect of delayed bifurcation is explained with the help of the model in Fig. 5.

Delayed bifurcation effect or memory effect associated with the slow passage of control parameter through Hopf bifurcation point is widely studied in the literature.^{40–43} When the control parameter is varied across the Hopf bifurcation point in a rate-dependent manner, the transition of the system dynamics from steady state to limit cycle oscillations gets delayed and occurs at a control parameter value greater than that at the Hopf bifurcation point. Such a delay in the transition of the system behavior is referred to as delayed bifurcation.

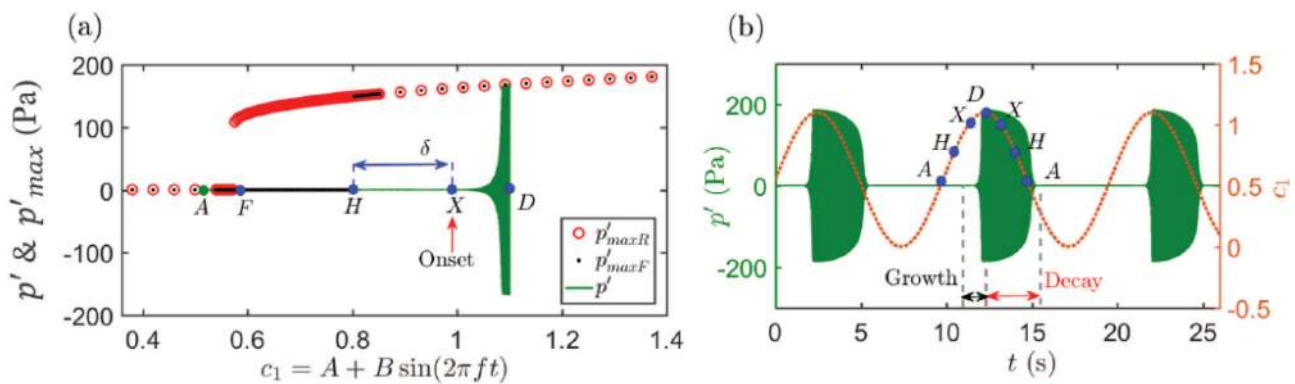


FIG. 5. (a) Transformed phase portrait of acoustic pressure oscillations (p') obtained from the standard model superposed on the bifurcation diagram of acoustic pressure (p'_{max}) obtained from quasi-static variation of c_1 . (b) The overlapped time series of the control parameter oscillations (c_1) and the acoustic pressure oscillations (p') during a state of bursting in the system, obtained from the model. Here, p'_{maxR} and p'_{maxF} refer to the reverse and the forward paths of quasi-static variation of c_1 . The point demarcated as A represents the mean value of c_1 .

For our model involving a slow–fast system, the delayed bifurcation due to slow parameter oscillations can be depicted using a “transformed phase portrait.”⁴² The transformed phase portrait is a plot of the time evolution of the acoustic pressure oscillations (the fast subsystem variable) with respect to the time-varying control parameter c_1 (the slow subsystem variable), as shown in Fig. 5(a). For clarity, we plot the acoustic pressure oscillations on the transformed phase diagram starting from the point A [Fig. 5(a)], where the pressure fluctuations are in the rest state [Fig. 5(a)] to the point where the pressure fluctuations achieve the maximum amplitude of periodic oscillations (at point D), observed during the onset of burst in a signal [Fig. 5(b)]. We then superimpose this transformed phase portrait on the bifurcation diagram, which is obtained by plotting the variation of the maximum amplitude of the acoustic pressure oscillations with respect to the quasi-static variation of the control parameter [Fig. 5(a)].

We note that the delay associated with the occurrence of the first burst depends on the initial conditions [i.e., $\eta(0)$] of the acoustic pressure fluctuations. However, the delay associated with the subsequent bursts in the same signal is independent of initial conditions for fixed values of A , B , and f [in Eq. (9)] for the oscillating parameter c_1 .⁴¹ Hence, the transformed phase portrait is obtained from any subsequent burst after disregarding the first burst as a transient. In Fig. 5(a), we show the transformed phase portrait for the case when the control parameter oscillates with an amplitude of $B = 0.55$ with a frequency $f = 0.102$ Hz about a mean value $A = 0.55$. Furthermore, we show the overlapped time series of slow control parameter oscillations and fast acoustic pressure oscillations during the state of bursting in the system in Fig. 5(b). Points A, F, H, X, and D are the reference points of c_1 on the bifurcation diagram in Fig. 5(a) corresponding to the demarcations on the time series in Fig. 5(b). Consider the oscillation of the control parameter starting from the mean value, indicated by the point A in Figs. 5(a) and 5(b). We define the forward oscillation from point A to point D and the reverse oscillation from point D to point A in half a cycle of the control parameter oscillation [Fig. 5(b)].

Even as the control parameter oscillations cross the Hopf bifurcation point H, we observe steady state dynamics in acoustic pressure (p'), i.e., the transition of p' from the rest to the active state does not occur immediately at H [Fig. 5(a)]. Such a transition occurs only at a value of c_1 that is greater than that at H, i.e., at point X. The identification of the exact point of the onset of the growth of oscillations (i.e., point X) is non-trivial and is described in detail in Appendix A. We qualitatively indicate the delayed bifurcation in the system by what we define as the “delay value” (in terms of c_1), henceforth referred to as δ . The delay value (δ) represents the difference in the values of c_1 at point H (the Hopf point) and at point X (where the onset of a burst of periodic oscillations occurs in the acoustic pressure signal).

In the forward direction, when the value of c_1 grows from point A to D [Fig. 5(b)], we obtain periodic oscillations in the p' signal only when the value of c_1 traverses from point X to D on the bifurcation plot [Fig. 5(a)]. In the reverse path of c_1 (i.e., from point D to A), the value of p'_{max} continuously decreases from point D to F [Fig. 5(a)] corresponding to which the amplitude of the p' oscillations in the burst also decreases. Once the control parameter crosses the fold point F, the periodic oscillations of p' in the burst

decay rapidly to the rest state. Hence, the dynamics of p' is sustained on a longer stretch of the stable limit cycle branch in the reverse direction of the control parameter oscillation as compared to the forward direction. As a result, the growth and the decay pattern of the bursts are asymmetric.

In addition, we investigate the effect of slow parameter oscillations across a supercritical Hopf bifurcation, which does not have a hysteresis zone, using a similar model. The corresponding equations and results are discussed in Appendix B. In a supercritical Hopf bifurcation, the amplitude of limit cycle oscillations increases gradually from the rest state and there is no sudden jump in the value of p'_{max} . We find that the slow parameter oscillations across the supercritical Hopf bifurcation induce bursts of periodic oscillations amidst nearly quiescent state with distinct growth and decay pattern. Since there is a delay associated with the transition of dynamics from steady state to periodic oscillations, there is a steep rise in the amplitude of the acoustic pressure signal, that is, a sudden growth of high-amplitude periodic oscillations (refer Fig. 11). During the reverse oscillation, the amplitude of periodic oscillations decreases gradually to the rest state.

D. Factors effecting the delayed bifurcation

In this section, we present the effect of the change in the mean value, amplitude, and frequency of the control parameter oscillations on the delay value (represented as δ in Fig. 5) and also on the characteristics of bursting oscillations, using the model, through Fig. 6.

In the transformed phase diagrams in Fig. 6, points F and H indicate the fold and the Hopf points, respectively. We consider two cases in Figs. 6(a) and 6(b) where for case I, $A_I = 0.55$, and for case II, $A_{II} = 0.85$, while $B = 0.55$, $f = 0.102$ Hz in both cases. From the transformed phase diagram in Fig. 6(a), we observe that an increase in A leads to a corresponding increase in the delay value (δ), i.e., if $A_I < A_{II}$ then $\delta_I < \delta_{II}$. The time series of the acoustic pressure for both the cases are overlapped and plotted in Fig. 6(b) for the ease of comparison. From Fig. 6(b), we infer that as A increases, the epochs of high-amplitude periodic oscillations (i.e., burst) increase and the epochs of low-amplitude aperiodic fluctuations correspondingly decrease in the p' signal. The maximum amplitude of the periodic oscillations in the p' signal also increases with an increase of A . This is expected from the bifurcation diagram, where we see an increase in the amplitude of limit cycle oscillation with the increase in the value of the control parameter. Since the value of A_I is lesser than A_{II} , for the same amplitude B , the maximum amplitude achieved along the limit cycle branch is greater for case II.

Next, we inspect the effect of variation in the frequency (f) of the control parameter oscillations while its amplitude (B) and mean value (A) are kept constant in Figs. 6(c) and 6(d). Two cases are considered as before, case I: $f_I = 0.102$ Hz and case II: $f_{II} = 0.238$ Hz, while the amplitude and mean value of c_1 for both cases are fixed at $B = 0.55$ and $A = 0.85$, respectively. We note that as f increases, the number of bursts occurring in the signal in a fixed duration also increases [Fig. 6(d)]. Furthermore, from the transformed phase portrait in Fig. 6(c), it is clear that the delay value (δ) associated with the onset of bursts increases corresponding to the increase in f . This means, if $f_I < f_{II}$, then $\delta_I < \delta_{II}$. We also note that the maximum

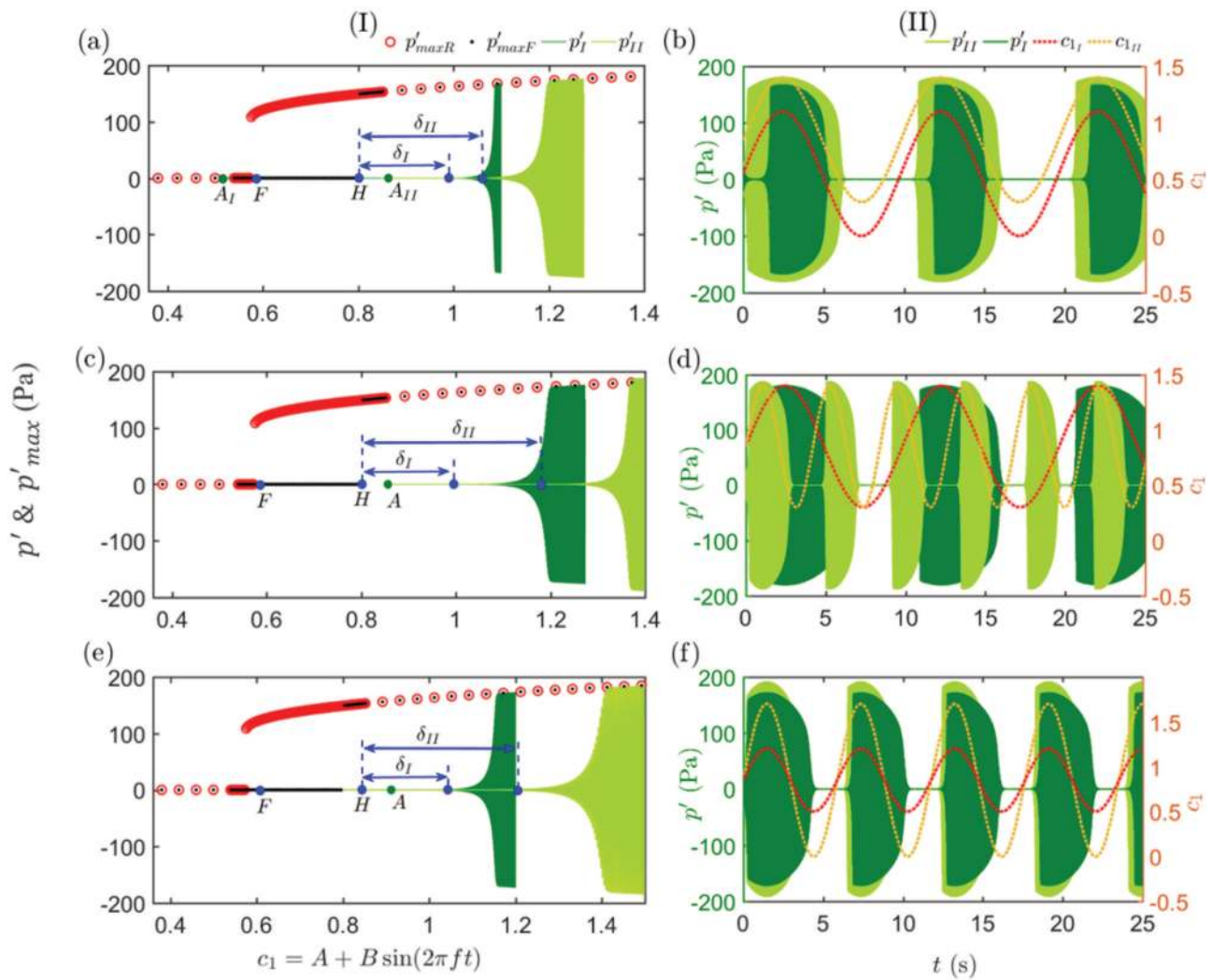


FIG. 6. (I) Transformed phase diagrams and (II) the corresponding overlapped time series of the control parameter oscillations and the acoustic pressure oscillations obtained from the model, for the cases shown in [(a) and (b)] with different mean values A_I and A_{II} while B and f are fixed, [(c) and (d)] with different frequencies f_I and f_{II} , while A and B are fixed, and [(e) and (f)] with different amplitudes B_I and B_{II} while A and f are fixed. The point demarcated as A represents the mean value of c_1 .

amplitude of the burst remains nearly the same with an increase in f at fixed values of A and B .

Finally, in Figs. 6(e) and 6(f), we study the effect of variation of the amplitude (B) of the control parameter oscillations while keeping A and f constant. Again, we consider two cases, case I: $B_I = 0.35$ and case II: $B_{II} = 0.85$ for fixed values of $A = 0.85$ and $f = 0.17$ Hz. We find that the maximum amplitude of acoustic pressure oscillations in the burst is directly proportional to the amplitude of the control parameter oscillations. We also note that an increase in B does not affect the epoch of a burst observed in the signal, i.e., the duration of bursts remains the same [Fig. 6(f)]. Further, from the transformed phase portrait in Fig. 6(e), we note that the delay value (δ) is higher for case II, i.e., if $B_I < B_{II}$ then $\delta_I < \delta_{II}$.

V. INVESTIGATING THE INTERDEPENDENCE OF SLOW AND FAST SUBSYSTEMS USING MODEL

In Sec. IV, we discussed the case where the externally introduced slow-scale oscillations in the control parameter are independent of the dynamics of the fast scale oscillations observed in the acoustic pressure. However, in practical thermoacoustic systems, the acoustic, hydrodynamic, and flame fluctuations, which ensue at distinct timescales, are non-linearly coupled⁴⁴ and the quantification of the effect of each subsystem on the other is difficult. For instance, there is an inevitable dependence between the evolution of the acoustic pressure fluctuations and various control parameters, viz., equivalence ratio, mixing, and burning rates, temperature, etc., inherent to the governing system. In addition, there is a

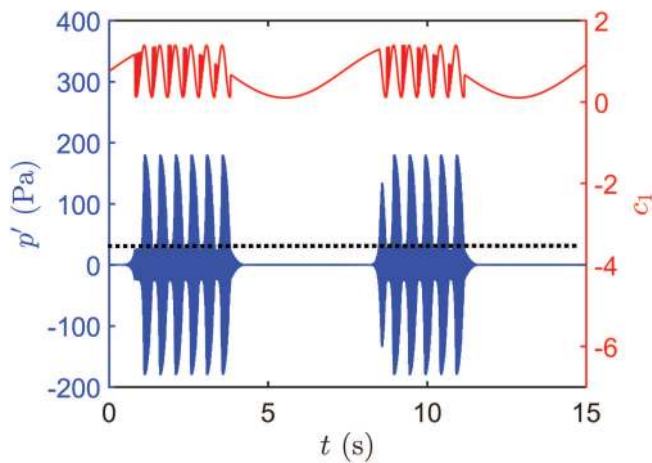


FIG. 7. Schematic representation of the simultaneous evolution of the acoustic pressure (p' , in blue) and the control parameter (c_1 , in red) oscillations obtained through the modified model. The dotted line represents the chosen threshold of $p'_{th} = 25$ Pa (which is around 15% of the maximum amplitude); if $p'_{env} > p'_{th}$, frequency of the control parameter (c_1) oscillation is $f = 0.17$ Hz; if $p'_{env} < p'_{th}$, then $f = 15 \times 0.17$ Hz. The frequency of the acoustic pressure oscillations is 170 Hz. The noise intensities are $\sigma_a = 0.0001$ and $\sigma_m = 0$.

possible interdependence between the underlying turbulence intensity and the dynamics of acoustic variables. The dynamics arising in the system due to the interaction between the subsystems with multiple timescales is highly complex. Therefore, in this section, we intend to probe the occurrence of bursting dynamics in the acoustic field due to such interdependence of the slow and fast subsystems through the model. To model the interaction between the various subsystems of a thermoacoustic system, we present two approaches: (I) by coupling the slow and fast subsystems in the presence of low-intensity noise and (II) by introducing noise (additive and multiplicative) in the absence of slow oscillations in the control parameter.

A. Effect of coupling the slow and fast subsystems

From our experiments in the Rijke tube, we understand that bursts of periodic oscillations arise in the acoustic pressure fluctuations (fast subsystem) as a result of slow oscillations of a control parameter (slow subsystem). Further, we notice that when the slow and the fast oscillations are uncoupled, the bursts occur at equal intervals in the acoustic pressure signal. However, in practical combustors, such bursts occur at random intervals in the signal. Sometimes, such bursts also possess a peculiar feature of periodic modulation in the amplitude envelope of the active state in the acoustic pressure signal^{18,45} [as shown in Fig. 8(a)], known as amplitude modulated bursting.

“Amplitude modulated bursting” is a known phenomenon in the studies pertaining to slow–fast systems.^{46,47} As discussed by Han *et al.*,⁴⁷ amplitude modulated bursting is characterized by modulations in the envelope of the active phase of bursting. They show

that amplitude modulated bursting can occur in the system dynamics due to “multi-frequency slow parametric modulation,” that is, if there exist multiple slow frequencies in the parameter modulations when the system undergoes a Hopf bifurcation or any other type of bifurcation. In our approach using the modified model, the system has only one frequency that is a function of time, which introduces amplitude modulated bursting.

We speculate that amplitude modulated bursting in the acoustic pressure signal may arise as a result of interactions between the slow and the fast subsystems in a combustor. Therefore, to study the interdependence of these two subsystems, we modify the standard model by making the frequency of the control parameter oscillations dependent on the amplitude of the fast oscillations in the acoustic pressure. Due to such interdependence, we assume that the frequency of the control parameter oscillations increases to a higher value during the active state of the burst as compared to that during the rest state. We subsequently show that such an assumption models the amplitude modulated bursting observed in laboratory-scaled combustors. In order to realize this altering frequency in the model, we numerically capture the amplitude envelope of the acoustic pressure fluctuations as and when the system evolves [see Fig. 7]. Then, we choose a threshold of acoustic pressure amplitude, p'_{th} , which is a suitable fraction of the amplitude of the limit cycle oscillations. The choice of p'_{th} is based on examining several threshold values in the model and is restricted to be around 10%–30% of the maximum amplitude of acoustic pressure oscillations (depending on the level of noise used in the system). If the value of the threshold is higher than 30%, we observe bursting dynamics only for a very small range of the control parameter. If the amplitude envelope of the acoustic pressure oscillations is below p'_{th} , the frequency of c_1 is chosen to be f , whereas, if the amplitude envelope of acoustic pressure oscillations is above p'_{th} , the frequency of c_1 is chosen to be a multiple of f . Figure 7 represents the simultaneous evolution of c_1 and p' when the frequency of c_1 is allowed to vary according to the amplitude of p' as described. We, henceforth, refer to the model with such interdependence between the slow and the fast subsystems as the “modified model.” In a thermoacoustic system, the evolution of dynamics of each subsystem is dependent on that of the other subsystems. As a result, the interaction of some slow subsystems with the fast subsystem may give rise to perturbations in various other slow subsystems. Thus, there may be frequency variations in parameters associated with different subsystems other than the control parameter originally oscillating at a slow timescale. However, the cumulative effect of the interaction of all these slow subsystems will be reflected in the heat release rate fluctuations. Hence, in the modified model, we account for the interactions between the various slow and fast subsystems through the frequency variation of a single parameter c_1 , which eventually affects the heat release rate oscillations according to Eq. (8).

B. Effect of additive and multiplicative noise

To model the interactions between the various subsystems (hydrodynamics, acoustics, and flame dynamics), a completely different approach may be identified, in which we disregard the approach using slow timescale oscillations of the control parameter. In this second approach, we model such interactions using a

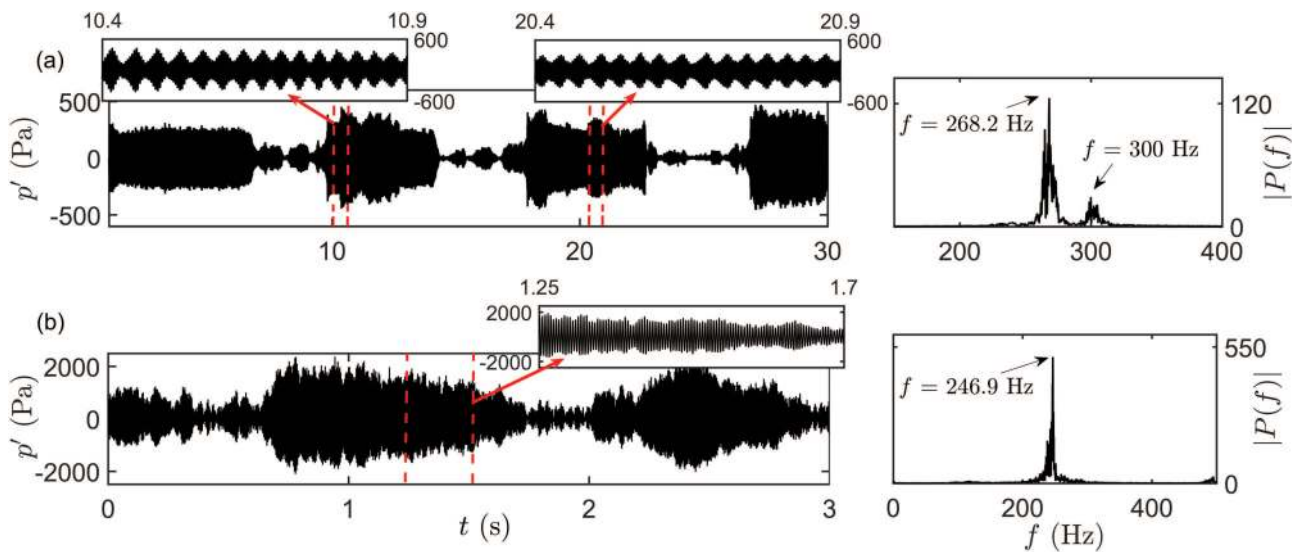


FIG. 8. Time series of the acoustic pressure oscillations and corresponding amplitude spectrum observed during the state of intermittency prior to thermoacoustic instability in (a) spray combustor¹⁸ ($Re \approx 2.6 \times 10^3$) and (b) turbulent combustor⁹ ($Re \approx 1.4 \times 10^4$). The insets show small epochs of periodic oscillations during bursts where the inset of (a) shows regular amplitude modulations in the envelope and the inset of (b) highlights irregularly modulated envelope of the acoustic pressure oscillations.

combination of additive and multiplicative noise. According to Eq. (9), the multiplicative noise introduces dependence between the non-coherent heat release rate (\dot{q}_{nc}) and the instantaneous value of the acoustic pressure oscillations in the system. Thus, the multiplicative noise aids in capturing the nonlinear interaction between the acoustic subsystem (pressure oscillations) and the heat release rate oscillations in the combustor. Further, the additive noise term in Eq. (9) helps to model the effect of turbulence (hydrodynamic subsystem) on the heat release rate fluctuations.⁴⁸ Thus, a combination of additive and multiplicative noise is used to model the interaction between the various subsystems of a combustor. When such a combination of additive and multiplicative noise is introduced in the model, we observe bursting behavior when the control parameter is in the vicinity of the Hopf bifurcation point.

First, we show the intermittency signals and the corresponding amplitude spectra observed prior to thermoacoustic instability in two laboratory-scaled combustors, which have been discussed earlier by Pawar *et al.*¹⁸ [Fig. 8(a)] and Nair *et al.*⁹ [Fig. 8(b)]. Next, we compare the time series and the amplitude spectra of the intermittent oscillations in the acoustic pressure signals obtained from the model using the two approaches, namely, (i) the modified model [Fig. 9(a)] and (ii) the introduction of additive and multiplicative noise in the model [Fig. 9(b)]. Finally, we compare the features of intermittent bursts obtained from model [Fig. 9] with that observed through experiments [Fig. 8].

Figure 8(a) delineates the intermittency signal from a low-turbulence spray combustor where we observe distinct amplitude modulated bursting in the signal and also the occurrence of a sideband frequency in the amplitude spectrum of the acoustic pressure oscillations.¹⁸ The corresponding amplitude spectrum has a

dominant frequency peak at 268.2 Hz and a sideband frequency at 300 Hz. These features, in turn, indicate the presence of multiple frequencies in the slow subsystems of the combustor.

Similarly, Fig. 8(b) illustrates the intermittent oscillations in the acoustic pressure signal obtained prior to thermoacoustic instability in a laboratory-scale bluff-body stabilized turbulent combustor.⁹ The amplitude envelope of the pressure signal has very small and irregular modulations during the high-amplitude bursts of periodic oscillations. The amplitude spectrum of this signal shows a single dominant peak around a frequency of 246.9 Hz. This could happen if the nonlinear interaction of the slow and the fast subsystems is incapable of introducing multiple slow frequencies in the system in the presence of dominant turbulent flow fluctuations.

In order to replicate the feature of amplitude modulated bursting as observed in a laboratory-scale spray combustor [Fig. 8(a)], we use the modified model described in Sec. V A. Figure 9(a) shows the intermittent oscillations obtained from the modified model when the value of p'_{th} is approximately 15% of the maximum amplitude of the acoustic pressure oscillations. It is assumed that the control parameter oscillates at a base frequency of 0.17 Hz when the pressure amplitude is below the threshold, while the frequency of the control parameter increases to 8.5 Hz otherwise. Here, we use additive noise alone, i.e., $\sigma_m = 0$ and $\sigma_a = 0.1$. With this approach, we obtain an intermittency signal where the acoustic pressure oscillations switch between high-amplitude periodic oscillations and low-amplitude aperiodic fluctuations [Fig. 9(a)]. Moreover, the occurrence of bursts is not periodic, owing to the fact that the frequency of the slowly oscillating control parameter varies as per the acoustic pressure oscillations which is influenced by the presence of noise in the acoustic field. This is different from the periodically occurring bursts we

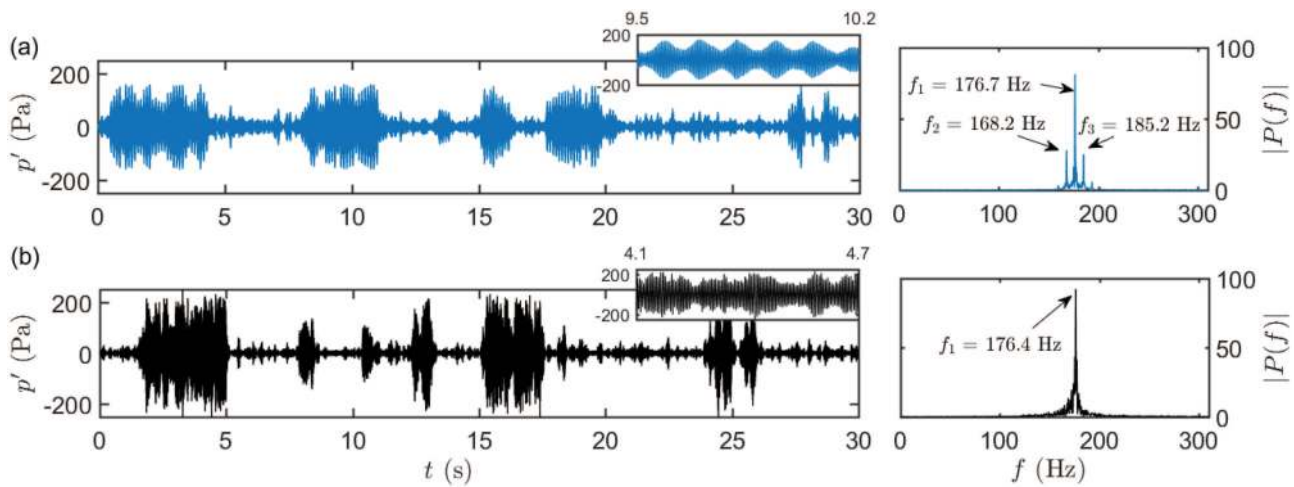


FIG. 9. (a) The intermittency signal obtained from the modified model when the pressure threshold is set at $p'_{th} = 25$ Pa. If $p'_{env} < p'_{th}$, frequency of oscillating control parameter c_1 is $f = 0.17$ Hz, while if $p'_{env} > p'_{th}$, then $f = 8.5$ Hz with noise strengths $\sigma_a = 0.1$ and $\sigma_m = 0$. (b) The intermittency signal obtained from introducing additive and multiplicative noise of strengths $\sigma_a = 0.05$ and $\sigma_m = 0.2$, respectively, in the model. The amplitude spectra corresponding to periodic oscillations of each time series shown in the insets are plotted in the right column.

observed in Fig. 4, when the slow and the fast subsystems were not coupled.

The inset of Fig. 9(a) shows regular modulations in the amplitude envelope of the acoustic pressure oscillations, which is known as amplitude modulated bursting. The corresponding amplitude spectrum has one dominant peak at the natural frequency of the acoustic field (176.7 Hz) and two sideband frequency peaks at 168.2 Hz and 185.2 Hz. Here, the frequency difference of 8.5 Hz between the dominant frequency and the sideband frequencies is equal to the value of the frequency of the slow oscillations (i.e., 8.5 Hz) introduced in the control parameter, when the amplitude envelope of pressure oscillations is above the designated threshold. This is also the frequency of the modulations in the amplitude envelope of the pressure oscillations during bursts of periodic oscillations. This behavior reasserts that the presence of multiple slow frequencies of control parameter oscillations is responsible for amplitude modulated bursting, and the higher of these multiple slow frequencies is reflected in the modulations of the amplitude envelope of acoustic pressure during bursts. Such a signal closely replicates the features of the amplitude-modulated limit cycle oscillations observed by Boudy *et al.*⁴⁵ in a multiple flame premixed burner and the amplitude-modulated intermittent oscillations seen in a low-turbulence laboratory-scale spray combustor¹⁸ [as shown in Fig. 8(a)].

On the other hand, Fig. 9(b) shows the intermittency signal obtained from the combination of additive and multiplicative noise alone (i.e., without the slow oscillations in the control parameter) in the model [refer to Eq. (9)]. Here, we choose the noise intensities such that $\sigma_a < \sigma_m$, since we expect that in low-turbulence systems, the acoustic pressure dynamics would be more strongly influenced by the interaction of the heat release rate and the acoustic pressure oscillations as compared to the effect of turbulent fluctuations.

Switching of the acoustic pressure oscillations between periodic and aperiodic oscillations in the presence of noise is obtained when the control parameter value is close to the Hopf bifurcation point. Similar to the previous approach using the modified model, this approach also produces bursts of periodic oscillations at irregular intervals. Furthermore, we observe that the amplitude envelope of the acoustic pressure oscillations has small and irregular amplitude modulations during bursts. The amplitude spectrum corresponding to periodic oscillations in the burst shows only a single dominant peak at 176.4 Hz and no sideband frequencies. Moreover, if we use $\sigma_a > \sigma_m$, this approach can also produce intermittent bursting similar to that observed experimentally in the intermittency signals obtained from a highly turbulent combustor⁹ such as that shown in Fig. 8(b). Thus, the introduction of additive and multiplicative noise alone in the model aids in capturing the occurrence of bursts in the acoustic field of the combustor. However, unlike the modified model, this approach does not capture the feature of regular amplitude-modulated bursting as shown in Fig. 9(a).

From comparing our results discussed in Figs. 9(a) and 9(b), we can postulate to some extent the physical cause of the bursting behavior observed during intermittency in different combustors. Thermoacoustic systems, which show amplitude-modulated bursting, i.e., regular modulations in the limit cycle oscillations or the existence of sideband frequencies along with a dominant peak at the natural frequency in the amplitude spectrum, are likely to have strongly interacting slow and fast subsystems. On the other hand, if the bursting dynamics portrays irregular modulations in the amplitude of bursts or the envelope of limit cycles or a single dominant frequency peak in the amplitude spectrum, then the system dynamics might be predominantly controlled by the underlying flow fluctuations (background turbulence) and its influence on other various subsystems.

VI. CONCLUSIONS

In this work, we investigated experimentally and theoretically the role of multiple timescales in the occurrence of bursting dynamics during intermittency in a thermoacoustic system. We conduct experiments on a horizontal Rijke tube and theoretical investigations through a model, each exhibiting subcritical Hopf bifurcation. Bursting dynamics is obtained when the control parameter oscillates at low frequencies about a mean value in the bistable zone of subcritical Hopf bifurcation. In order for sustained bursting dynamics to occur, the amplitude of the control parameter oscillations must be such that these oscillations necessarily cross the Hopf bifurcation point to overcome delayed bifurcation. When the slow and fast subsystems are independent of each other, we obtain bursting at regular intervals and the bursts are asymmetric. Through a model, we explain that the growth and decay patterns are different due to the delayed bifurcation associated with slow oscillations of the control parameter around the Hopf bifurcation point. We showed that the delayed bifurcation of the acoustic pressure fluctuations with respect to the oscillating control parameter is dependent on the frequency, the amplitude, and the mean value of the oscillating control parameter.

Further, we present two approaches to model the interaction between the various subsystems. In the first approach, we introduce a coupling between the frequency of the slowly oscillating control parameter and the amplitude envelope of the fast oscillating acoustic pressure in the system. In the second approach, we model the interactions of various subsystems using noise which produces bursts of periodic oscillations with irregular amplitude modulations. The interactions between the subsystems of a thermoacoustic system may be influenced more by either multiple timescales or the underlying flow fluctuations, depending on the experimental conditions. We, thus, provide a possible explanation to various features of bursting oscillations observed during intermittency in thermoacoustic systems.

ACKNOWLEDGMENTS

We acknowledge financial support from the Office of Naval Research Global and Contract Monitor (Dr R. Kolar) (Grant No. N62909-14-1-N299). We would also like to acknowledge financial support from the J. C. Bose Fellowship (No. JCB/2018/000034/SSC).

APPENDIX A: DETECTION OF THE ONSET OF THE ACTIVE STATE OF BURST IN THE PARAMETER SPACE

In Sec. IV C, we discussed the delayed bifurcation effect caused by the slow passage of control parameter via Hopf bifurcation. As noted earlier, the choice of the onset point (X) corresponding to the onset of periodic oscillations from the steady state is non-trivial. Here, we describe the manner in which we detect the point X with the help of an example. Consider control parameter (c_1) oscillations about a mean value of $A = 0.8$ with an amplitude $B = 0.4$ and frequency $f = 0.17$ Hz. Figure 10(a) shows the pressure oscillations while Fig. 10(b) shows the amplitude envelope of the corresponding pressure oscillations plotted on a log scale as a function of the control parameter oscillations. Despite minute oscillations, we see a sudden change in the slope of the log of the envelope of pressure

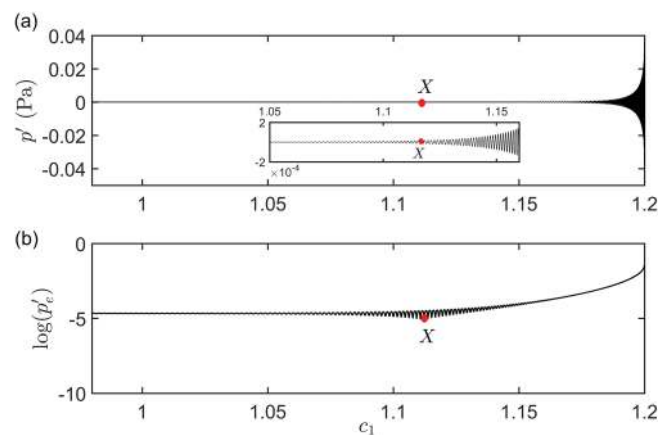


FIG. 10. (a) The variation of acoustic pressure oscillations (p') and (b) log of the amplitude envelope of these pressure oscillations (p'_e) as a function of the time-varying control parameter (c_1) during the growth of amplitude of the burst. The values of parameters are: $A = 0.8$, $B = 0.4$, $f = 0.17$ Hz, and $\sigma_a = 0.0001$ while $\sigma_m = 0$.

fluctuations in Fig. 10(b). Such sudden change of the pressure amplitude in the log-scale delineates the starting of exponential growth of amplitude, which thus demarcates the point of the onset of a burst of periodic oscillations in the signal and we choose this point as X in our analysis. Thus, the plot of pressure amplitude on a log-scale helps in identifying the onset of burst in the signal, which is otherwise not evident from the plot of pressure oscillations in Fig. 10(a).

APPENDIX B: DELAYED BIFURCATION DUE TO SLOW OSCILLATIONS ACROSS A SUPERCRITICAL HOPF BIFURCATION

In Fig. 11, we show the effect of slow oscillations in the control parameter across a supercritical Hopf bifurcation. The bifurcation diagram is obtained from quasi-static variation of the control parameter c_1 , when the coherent heat release term is modeled by the canonical form of supercritical Hopf bifurcation, as given in Eq. (B1) in the standard model [instead of Eq. (8)],

$$\dot{q}'_c = -c_1(\eta - \tau\dot{\eta}) + c_3(\eta - \tau\dot{\eta})^3. \quad (\text{B1})$$

Figure 11(a) shows the transformed phase portrait for the case when the control parameter oscillates with an amplitude of $B = 0.65$, and frequency $f = 0.17$ Hz about a mean value $A = 0.7$. Figure 11(b) shows the overlapped time series of oscillations of c_1 and p' during the bursting state in the system. Reference point A demarcates the starting point of oscillation of c_1 , H demarcates the Hopf bifurcation point of the supercritical bifurcation, which occurs at $c_1 = 0.79$, X demarcates the onset point of the burst, and D demarcates the point at which c_1 achieves a maximum value in an oscillation cycle. Clearly, slow oscillations of the control parameter across the supercritical Hopf bifurcation point introduce a delayed bifurcation as observed for subcritical Hopf bifurcation earlier in Fig. 5.

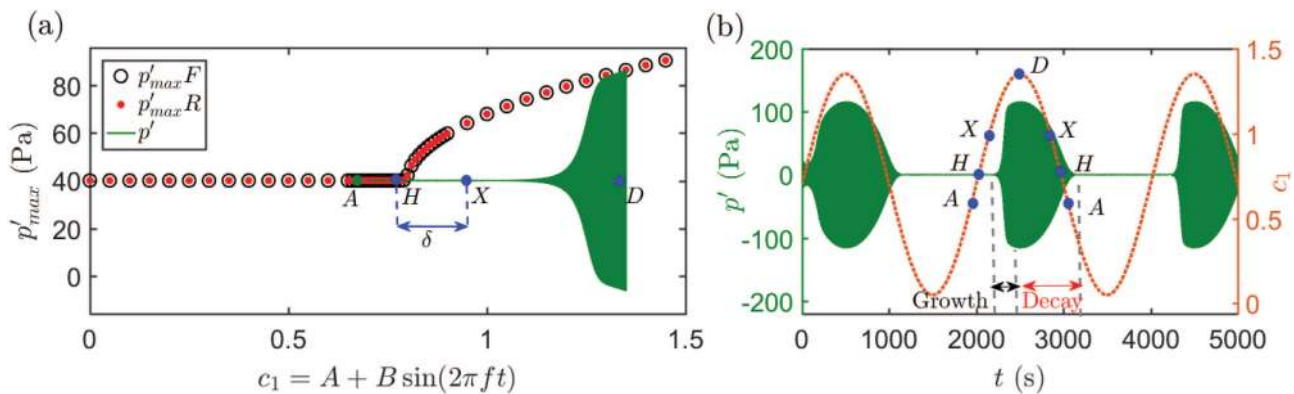


FIG. 11. (a) Transformed phase portrait of acoustic pressure oscillations obtained from the standard model for supercritical bifurcation superposed on the bifurcation diagram of acoustic pressure (p'_{max}) obtained from quasi-static variation of c_1 . (b) The overlapped time series of the control parameter oscillations (c_1) and the acoustic pressure oscillations (p') during a state of bursting in the system.

As compared to the subcritical Hopf bifurcation, a supercritical bifurcation does not have a hysteresis zone and the amplitude of the limit cycle oscillations increases gradually from the steady state [Fig. 11(a)]. The dynamics of the system transitions from the steady state to limit cycle oscillations after a delayed bifurcation, and, therefore, there is a sudden jump in the amplitude of the pressure oscillations during the onset of a burst. In the reverse path, the amplitude of periodic oscillations decreases gradually along the limit cycle branch and the pressure oscillations eventually attain a rest state. The growth and decay patterns are thus different, even when the system undergoes a supercritical bifurcation. The effect of varying the amplitude, the frequency, and the mean value of the oscillating parameter across a supercritical Hopf bifurcation is similar to that which is discussed for the case of subcritical Hopf bifurcation in Sec. IV D.

We note a subtle difference between the decay pattern of the bursts that occur in the case of a subcritical and a supercritical bifurcation. The decay of the oscillations in a burst caused in a system having subcritical bifurcation is initially gradual, as the control parameter oscillations move along the limit cycle branch. However, as the control parameter crosses the fold point, there is a sharp decay in the pressure oscillations in the burst. For a system exhibiting supercritical bifurcation, the decay in pressure oscillations in a burst is always gradual as the control parameter oscillations trace the continuous limit cycle branch into the steady state regime.

DATA AVAILABILITY

The data that support the findings of this study are available from the corresponding author upon reasonable request.

REFERENCES

- 1 F. Culick and P. Kuentzmann, "Unsteady motions in combustion chambers for propulsion systems," Technical Report (Nato Research and Technology Organization Neuilly-SUR-SEINE, France, 2006).
- 2 R. Sujith, M. Juniper, and P. Schmid, "Non-normality and nonlinearity in thermoacoustic instabilities," *Int. J. Spray Combust. Dyn.* **8**, 119–146 (2016).

- 3 J. W. Strutt and B. Rayleigh, *The Theory of Sound* (Dover, 1945).
- 4 M. P. Juniper and R. I. Sujith, "Sensitivity and nonlinearity of thermoacoustic oscillations," *Annu. Rev. Fluid Mech.* **50**, 661–689 (2018).
- 5 R. Sujith and V. R. Unni, "Complex system approach to investigate and mitigate thermoacoustic instability in turbulent combustors," *Phys. Fluids* **32**, 061401 (2020).
- 6 T. C. Lieuwen, "Experimental investigation of limit-cycle oscillations in an unstable gas turbine combustor," *J. Propul. Power* **18**, 61–67 (2002).
- 7 N. Ananthkrishnan, S. Deo, and F. E. Culick, "Reduced-order modeling and dynamics of nonlinear acoustic waves in a combustion chamber," *Combust. Sci. Technol.* **177**, 221–248 (2005).
- 8 F. Culick, "Some recent results for nonlinear acoustics in combustion chambers," *AIAA J.* **32**, 146–169 (1994).
- 9 V. Nair, G. Thampi, and R. I. Sujith, "Intermittency route to thermoacoustic instability in turbulent combustors," *J. Fluid Mech.* **756**, 470–487 (2014).
- 10 H. Gotoda, Y. Shinoda, M. Kobayashi, Y. Okuno, and S. Tachibana, "Detection and control of combustion instability based on the concept of dynamical system theory," *Phys. Rev. E* **89**, 022910 (2014).
- 11 V. R. Unni and R. I. Sujith, "Flame dynamics during intermittency in a turbulent combustor," *Proc. Combust. Inst.* **36**, 3791–3798 (2017).
- 12 S. Domen, H. Gotoda, T. Kuriyama, Y. Okuno, and S. Tachibana, "Detection and prevention of blowout in a lean premixed gas-turbine model combustor using the concept of dynamical system theory," *Proc. Combust. Inst.* **35**, 3245–3253 (2015).
- 13 R. Delage, Y. Takayama, and T. Biwa, "On-off intermittency in coupled chaotic thermoacoustic oscillations," *Chaos* **27**, 043111 (2017).
- 14 S. Kheirkhah, J. M. Cirtwill, P. Saini, K. Venkatesan, and A. M. Steinberg, "Dynamics and mechanisms of pressure, heat release rate, and fuel spray coupling during intermittent thermoacoustic oscillations in a model aeronautical combustor at elevated pressure," *Combust. Flame* **185**, 319–334 (2017).
- 15 D. Ebi, A. Denisov, G. Bonciolini, E. Boujo, and N. Noiray, "Flame dynamics intermittency in the bistable region near a subcritical Hopf bifurcation," *J. Eng. Gas Turb. Power* **140**, 061504 (2018).
- 16 P. Kasthuri, V. R. Unni, and R. I. Sujith, "Bursting and mixed mode oscillations during the transition to limit cycle oscillations in a matrix burner," *Chaos* **29**, 043117 (2019).
- 17 F. Weng, S. Li, D. Zhong, and M. Zhu, "Investigation of self-sustained beating oscillations in a Rijke burner," *Combust. Flame* **166**, 181–191 (2016).
- 18 S. A. Pawar, R. Vishnu, M. Vadivukkarasan, M. Panchagnula, and R. I. Sujith, "Intermittency route to combustion instability in a laboratory spray combustor," *J. Eng. Gas Turb. Power* **138**, 041505 (2016).

- ¹⁹S. A. Pawar, A. Seshadri, V. R. Unni, and R. I. Sujith, "Thermoacoustic instability as mutual synchronization between the acoustic field of the confinement and turbulent reactive flow," *J. Fluid Mech.* **827**, 664–693 (2017).
- ²⁰N. Noiray, "Linear growth rate estimation from dynamics and statistics of acoustic signal envelope in turbulent combustors," *J. Eng. Gas Turb. Power* **139**, 041503 (2017).
- ²¹V. Nair and R. I. Sujith, "A reduced-order model for the onset of combustion instability: Physical mechanisms for intermittency and precursors," *Proc. Combust. Inst.* **35**, 3193–3200 (2015).
- ²²A. Seshadri, V. Nair, and R. I. Sujith, "A reduced-order deterministic model describing an intermittency route to combustion instability," *Combust. Theor. Model.* **20**, 441–456 (2016).
- ²³J. G. Hong, K. C. Oh, U. D. Lee, and H. D. Shin, "Generation of low-frequency alternative flame behaviors in a lean premixed combustor," *Energ. Fuel* **22**, 3016–3021 (2008).
- ²⁴C. Premchand, N. B. George, M. Raghunathan, V. R. Unni, R. I. Sujith, and V. Nair, "Lagrangian analysis of intermittent sound sources in the flow-field of a bluff-body stabilized combustor," *Phys. Fluids* **31**, 025115 (2019).
- ²⁵E. M. Izhikevich, "Neural excitability, spiking and bursting," *Int. J. Bifurcat. Chaos* **10**, 1171–1266 (2000).
- ²⁶Q. Bi, "The mechanism of bursting phenomena in Belousov-Zhabotinsky (BZ) chemical reaction with multiple time scales," *Sci. China Technol. Sci.* **53**, 748–760 (2010).
- ²⁷M. S. Yalin, in *River Mechanics* (Pergamon Press, 1992).
- ²⁸K. I. Matveev, "Thermoacoustic instabilities in the Rijke tube: Experiments and modeling," Ph.D. thesis (California Institute of Technology, 2003).
- ²⁹S. Mariappan and R. I. Sujith, "Modelling nonlinear thermoacoustic instability in an electrically heated Rijke tube," *J. Fluid Mech.* **680**, 511–533 (2011).
- ³⁰E. Gopalakrishnan and R. I. Sujith, "Influence of system parameters on the hysteresis characteristics of a horizontal Rijke tube," *Int. J. Spray Combust.* **6**, 293–316 (2014).
- ³¹E. Gopalakrishnan, J. Tony, E. Sreelekha, and R. I. Sujith, "Stochastic bifurcations in a prototypical thermoacoustic system," *Phys. Rev. E* **94**, 022203 (2016).
- ³²K. Balasubramanian and R. I. Sujith, "Thermoacoustic instability in a Rijke tube: Non-normality and nonlinearity," *Phys. Fluids* **20**, 044103 (2008).
- ³³M. P. Juniper, "Triggering in thermoacoustics," *Int. J. Spray Combust.* **4**, 217–237 (2012).
- ³⁴F. Nicoud and K. Wicczorek, "About the zero Mach number assumption in the calculation of thermoacoustic instabilities," *Int. J. Spray Combust.* **1**, 67–111 (2009).
- ³⁵B. T. Zinn and M. E. Loes, "Application of the Galerkin method in the solution of non-linear axial combustion instability problems in liquid rockets," *Combust. Sci. Technol.* **4**, 269–278 (1971).
- ³⁶J. D. Sterling, "Nonlinear analysis and modelling of combustion instabilities in a laboratory combustor," *Combust. Sci. Technol.* **89**, 167–179 (1993).
- ³⁷L. V. King, "XII. On the convection of heat from small cylinders in a stream of fluid: Determination of the convection constants of small platinum wires with applications to hot-wire anemometry," *Philos. Trans. A Math. Phys. Eng. Sci.* **214**, 373–432 (1914).
- ³⁸M. A. Heckl, "Active control of the noise from a Rijke tube," *J. Sound Vib.* **124**, 117–133 (1988).
- ³⁹P. M. Burrage, "Runge-Kutta methods for stochastic differential equations," Ph.D. thesis (University of Queensland, Australia, 1999).
- ⁴⁰S. M. Baer and E. M. Gaekel, "Slow acceleration and deceleration through a Hopf bifurcation: Power ramps, target nucleation, and elliptic bursting," *Phys. Rev. E* **78**, 036205 (2008).
- ⁴¹X. Han, Q. Bi, C. Zhang, and Y. Yu, "Study of mixed-mode oscillations in a parametrically excited Van der Pol system," *Nonlinear Dyn.* **77**, 1285–1296 (2014).
- ⁴²X. Han, F. Xia, P. Ji, Q. Bi, and J. Kurths, "Hopf-bifurcation-delay-induced bursting patterns in a modified circuit system," *Commun. Nonlinear Sci. Numer. Simul.* **36**, 517–527 (2016).
- ⁴³D. Premraj, K. Suresh, T. Banerjee, and K. Thamilmaran, "An experimental study of slow passage through Hopf and pitchfork bifurcations in a parametrically driven nonlinear oscillator," *Commun. Nonlinear Sci. Numer. Simul.* **37**, 212–221 (2016).
- ⁴⁴T. C. Liewwen, *Unsteady Combustor Physics* (Cambridge University Press, 2012).
- ⁴⁵F. Boudy, D. Durox, T. Schuller, and S. Candel, "Analysis of limit cycles sustained by two modes in the flame describing function framework," *Comptes Rendus Mécanique* **341**, 181–190 (2013).
- ⁴⁶T. Vo, M. A. Kramer, and T. J. Kaper, "Amplitude-modulated bursting: A novel class of bursting rhythms," *Phys. Rev. Lett.* **117**, 268101 (2016).
- ⁴⁷X. Han, M. Wei, Q. Bi, and J. Kurths, "Obtaining amplitude-modulated bursting by multiple-frequency slow parametric modulation," *Phys. Rev. E* **97**, 012202 (2018).
- ⁴⁸T. Liewwen and A. Banaszuk, "Background noise effects on combustor stability," *J. Propul. Power* **21**, 25–31 (2005).
- ⁴⁹T. C. Liewwen, "Statistical characteristics of pressure oscillations in a premixed combustor," *J. Sound Vib.* **260**, 3–17 (2003).
- ⁵⁰N. Noiray and B. Schuermans, "Deterministic quantities characterizing noise driven Hopf bifurcations in gas turbine combustors," *Int. J. Nonlin. Mech.* **50**, 152–163 (2013).
- ⁵¹S. A. Pawar, M. V. Panchagnula, and R. I. Sujith, "Phase synchronization and collective interaction of multiple flamelets in a laboratory scale spray combustor," *Proc. Combust. Inst.* **37**, 5121–5128 (2019).
- ⁵²J. M. Wilhite, B. J. Dolan, L. Kabiraj, R. Villalva Gomez, E. J. Gutmark, and C. O. Paschereit, "Analysis of combustion oscillations in a staged MLDI burner using decomposition methods and recurrence analysis," in *54th AIAA Aerospace Sciences Meeting* (AIAA, 2016), p. 1156.